CERN - EUROPEAN LABORATORY FOR PARTICLE PHYSICS

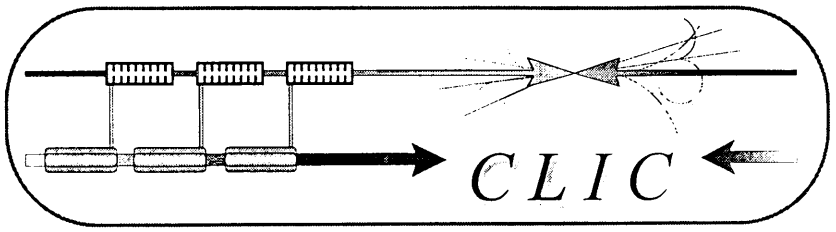

CERN/PS 99-014 (LP)
CLIC-Note-387

BEAM-BEAM SIMULATIONS WITH GUINEA-PIG

D. Schulte

Abstract

While the bunches in a linear collider cross only once, due to their small size they experience a strong beam-beam effect. GUINEA-PIG is a code to simulate the impact of this effect on luminosity and back ground. A short overview of the program is given with examples of its application to the back ground strudies for TESLA, the top quark threshold scan and a possible luminosity monitor, as well as some results for CLIC.

Presented at ICAP98, Monterey, CA., USA, September 1998

Geneva, Switzerland
15 April 1999

BEAM-BEAM SIMULATIONS WITH GUINEA-PIG

D. Schulte, CERN, CH-1211 Geneva 23,Switzerland

Abstract

While the bunches in a linear collider cross once only, due to their small size they experience a strong beam-beam effect. GUINEA-PIG is a code to simulate the impact of this effect on luminosity and background. A short overview of the program is given, with examples of its application to the background studies for TESLA, the top quark threshold scan and a possible luminosity monitor, as well as some results for CLIC.

1 INTRODUCTION

In future high-energy linear colliders, the beams have to be focused to very small sizes in order to achieve the required luminosity. The electro-magnetic field of each bunch will then have a strong effect on the other. In electron positron-collisions the resulting forces focus the two beams, leading to an enhancement of the luminosity. Due to the strong bending of their trajectories, the beam particles will emit high-energy photons, the so-called beamstrahlung. This significantly changes the luminosity spectrum and can lead to an increase in the background.

Electron-positron pairs can be produced in different processes during the collision. These particles can be low in energy and their trajectories are strongly affected by the beam fields. This has an important impact on the detector design in order to reduce the resulting background. Other sources of background are bremsstrahlung and the production of hadrons by the two-photon interaction.

The beam-beam interaction can only be partially treated analytically, simulations are therefore crucial. The code GUINEA-PIG [1] (Generator of Unwanted Interactions for Numerical Experiment Analysis—Program Interfaced to GEANT) is written in C and compiles with the GNU C-compiler. A copy of the code can be obtained from the author [2].

2 TRACKING ALGORITHMS

In the simulation, the beam particles are replaced typically by 20000 – 500000 macro-particles. The beams are cut longitudinally into a number of slices. Each slice of one beam interacts subsequently with each slice of the other beam. Since the particles are ultra-relativistic, the slice-slice interaction can be treated as a purely two dimensional problem using a clouds-in-cells method. The slice is transversely cut into cells, and the charge of the macro-particles is distributed onto this grid according to their position. The potentials on the grid points are then evaluated and from these the forces on the particles are derived.

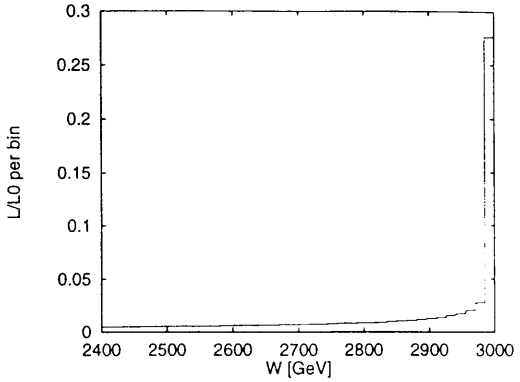

Figure 1: The luminosity spectrum for CLIC at $E_{cm} = 3\,\mathrm{TeV}$.

Calculating the potentials is one of the most time consuming operations, the simplest algorithm sums for each cell over all the others. Replacing the summation with a Fast Fourier Transformation increases the speed by a significant factor.

3 BEAMSTRAHLUNG

The bending of the beam-particle trajectories leads to the emission of photons (beamstrahlung). This effect is equivalent to synchrotron radiation. Instead of the critical energy E_c one commonly uses the beamstrahlung parameter $\Upsilon = 2/3 \cdot \langle E_c \rangle / E_0$ for its description, where E_0 is the nominal beam energy. The designs at 0.5–1 TeV centre-of-mass energy have usually $\Upsilon \ll 1$, which is called the classical regime. The fraction δ of its energy that a particle loses due to beamstrahlung is given in Table 1 for different designs. The number of photons emitted per beam particle is of the order of one. Therefore the discreteness of the process has to be taken into account. In the program, the produced photons are tracked and the corresponding electron-photon, positron-photon and photon-photon luminosities are calculated as well as the resulting background.

In CLIC at $E_{cm} = 3\,\mathrm{TeV}$ the beamstrahlung parameter will be much greater than one, i.e. $\Upsilon = 8.7$. The beamstrahlung is, in this regime, partly suppressed since the beam particles cannot emit photons with a higher energy than the particle has itself. The luminosity spectrum is shown in Fig. 1.

4 PAIR PRODUCTION

Electron-positron pairs can be produced by coherent and incoherent processes. For small Υ the incoherent processes

Table 1: Background levels for different collider designs. For TESLA the reference and high luminosity parameters (iL) are given. All designs have no crossing angle or use crab crossing.

		TESLA	TESLA iL	ILC	ILC	CLIC	CLIC	CLIC
E_{cm}	[GeV]	500	500	500	1000	500	1000	3000
f_{rep}	[Hz]	5	5	120	120	200	150	75
N_b		1130	2820	95	95	150	150	150
N	$[10^{10}]$	3.63	2.0	0.95	0.95	0.4	0.4	0.4
$\gamma\epsilon_x/\gamma\epsilon_y$	[μm]	14.0/0.25	10.0/0.03	4.5/0.1	4.5/0.1	1.88/0.1	1.48/0.07	0.6/0.01
β_x/β_y	[mm]	25/0.7	15/0.4	12/0.12	12/0.15	10/0.1	10/0.1	8/0.1
σ_x^*/σ_y^*	[nm]	845/18.9	554/4.95	332/4.95	235/3.9	196/4.52	123/2.7	40.4/0.58
σ_z	[μm]	700	400	120	120	50	50	30
Υ		0.03	0.04	0.10	0.29	0.18	0.56	8.7
$\mathcal{L}$	$[10^{33}\mathrm{cm}^{-2}\mathrm{s}^{-1}]$	6.0	31	6.54	12.9	6.3	13.6	133
δ	[%]	2.5	2.8	3.8	9.1	3.6	9.2	32
n_γ		2.0	1.65	1.16	1.5	0.8	1.1	2.15
$N_\perp$		31	44	9.8	18.4	2.9	8.0	128
N_H		0.13	0.23	0.07	0.33	0.022	0.15	8.0
N_{MJ}	$[10^{-2}]$	0.30	0.61	0.20	2.3	0.08	1.27	366

E_{cm}: centre-of-mass energy, f_{rep}: repetition frequency, N_b: number of bunches per train, σ: bunch dimensions at IP
N: number of particles per bunch, $\mathcal{L}$: actual luminosity, β: Beta functions at IP, $\gamma\epsilon$: normalised emittances,
Υ: Beamstrahlung parameter, δ: Average energy loss, n_γ: number of photons per beam particle,
$N_\perp$: Number of particles with $p_\perp > 20\,\mathrm{MeV}, \theta > 0.15$, N_{Hadr}: Hadronic events, N_{MJ}: Minijet pairs $p_\perp > 3.2\,\mathrm{GeV/c}$.

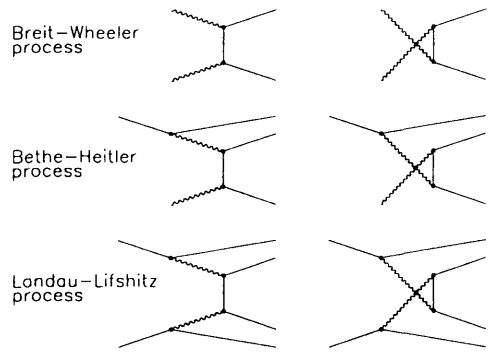

Figure 2: The incoherent pair production processes.

dominate. The three most important are called the Breit-Wheeler, the Bethe-Heitler and the Landau-Lifshitz processes, see Fig. 2. The last two can be derived from the first by the equivalent photon approximation. In this method, the initial beam-particle in the Feynmann diagrams are replaced by a spectrum of virtual photons. These photons are treated as being real as long as their virtuality remains below an upper limit. Above this limit they are ignored. In the program the lower boundary of the virtuality Q is given by $\tilde{Q}^2 = x^2m^2/(1-x)$. The upper limit $\hat{Q}^2$ can be chosen to be equal to the electron mass squared m^2 or to depend on the two-photon process. In the latter case either the transverse mass squared $m^2 + p_\perp^2$ of the final state or $s/4$ can be used as a scale. While the total cross section is not affected very much by the choice, the number of particles with large transverse momentum is. Comparisons of the Landau-Lifshitz process calculated with GUINEA-PIG and the Vermaseren Monte-Carlo show that using $\hat{Q}^2 = m^2$ significantly underestimates the number of tracks with transverse momenta of a few MeV [1]. The other two choices are in reasonable agreement but the number of tracks is still somewhat too small, since the imbalance of the transverse momenta of the final state particles is not simulated.

A small transverse momentum of the photon $q_\perp$ leads to a corresponding uncertainty in its transverse position [3]. If the beams are small enough the photon position can be outside of the beam. This effect was observed at VEPP4 [4] and HERA [5]. In the program it is treated by offsetting the photon with respect to the electron position by $b = \hbar/q_\perp$. The total number of pairs is reduced by a factor of about two. The effect on particles with larger angles and transverse momenta, which may enter the detector directly, is weaker.

In the program, the newly created particles are tracked through the fields of the two beams. Electrons which follow the direction of the electron beam are focused by the positron beam. The effective force of the electron beam is in this case small. The electrons which follow the positron beam are defocused by the electron beam and experience little effect from the positrons. The equivalent is true for positrons. In the program the step size of the particles is adjusted to their energy.

In the coherent pair-production process, a hard photon turns into an electron positron pair in a strong electromagnetic field. In the high beamstrahlung regime of CLIC at 3 TeV, the number of particles from this process is equal to several percent of the beam particles. Taking their contribution to the beam fields into account is therefore a necessary extension of the program to be made in the near future.

5 BREMSSTRAHLUNG

Another source of low energy particles is the bremsstrahlung process. In this case two beam-particles collide and one of them emits a hard photon. This process is implemented using the equivalent photon approach to replace one of the particles. One then has only to calculate the Compton process. The spectrum of the remnant beam-particles is relatively flat at the low energy end. The particles produced in this way always follow the beam with the same charge and are thus focused.

6 HADRONIC BACKGROUND

Two-photon collisions also lead to the production of hadrons. The photons interact in these cases not only as point-like particles but also with a certain probability as hadrons. The dependence of the total hadronic cross section on the centre-of-mass energy is thus comparable to that of the hadron-hadron interaction, even so its size is considerably smaller. In the program three different parametrisations can be used. The first is the upper estimate taken from Reference [7]

$$\sigma_H = 211\,\mathrm{nb}\cdot\left(\frac{s}{\mathrm{GeV}^2}\right)^{0.0808} + 297\,\mathrm{nb}\cdot\left(\frac{s}{\mathrm{GeV}^2}\right)^{-0.4525}$$

A second parametrisation used is taken from Reference [8] for comparison. The third is again from [7] us ing the expected cross section rather than the pessimistic case. In Table 1 the number of hadronic events N_H with a centre-of-mass energy in excess of 5 GeV is given for different collider designs. The first parametrisation is used.

A fraction of the hadronic events lead to the production of so-called minijets which have a significant transverse momentum. The simplest of the processes is the direct electro-magnetic production of a quark-anti-quark pair by the point-like photons. It differs from the pair production only by the charge and mass of the final state particles. It is also possible that one of the photons interacts hadronically. In this case a parton of this hadron collides with the other photon producing two jets. The remnants of the hadron form a third jet. If both photons interact as hadrons, two of these spectator jets are found. In total eleven cross sections have to be taken into account for the different quark, gluon and photon combinations.

In the program the real and virtual photons are replaced by spectra of partons for their hadronic interaction—very similar to the replacement of beam particles by virtual photons. The cross section for minijet production rises quickly at high photon-photon centre-of-mass energies. To calculate the cross section for events containing minijets one should take into account that the same hadron can produce more than one pair of minijets because more than one of its partons can scatter [9]. This however only affects the distribution of the minijets onto the hadronic events but not the rate itself. One would find fewer events with more jets each leading to the same total number of jets. This difficulty is ignored and each jet pair is assumed to be produced by a separate hadronic event—this should be a pessimistic approach.

Two parametrisations of the hadronic content of the photon are available in the program, one derived by Drees and Grassi [12], the other by Glück, Reya and Vogt [13]. The assumed values for the scale Λ_4 are adjusted automatically to the ones assumed by the authors.

In Table 1 the number of minijets N_{MJ} with a transverse momentum on the parton level of more than $p_\perp > 3.2\,\mathrm{GeV}$ is given. The second parametrisation is used.

The program produces two different files with hadronic output. The first contains the energies of two colliding photons that produce a hadronic event. The second contains the final-state four-vectors of the partons that produced minijets. The fragmentation can be done using PYTHIA [10] or an equivalent program.

7 BACKGROUND EFFECTS

Most of the particles from pair production have initially a small angle with respect to the beam axis. Their final angle depends mainly on the deflection by the beam fields. This leads to the distribution shown in Fig. 3 which shows a strong correlation between particle angle and maximal transverse momentum. The vast majority of the particles can be prevented from hitting the detector components by the combined effects of the longitudinal magnetic field of the detector and limited angular coverage. The solenoid field of the detector will limit the maximum distance a particle can reach from the beam axis depending on its transverse momentum. Particles with large transverse momenta however tend to have smaller angles and can be avoided by having a dead cone in the detector in the forward region.

Charged particles from the pair production that hit the vertex detector will cause background hits, making the reconstruction of the trajectories from physics events more difficult. Figure 4 shows the number of particles per bunch crossing that will hit the inner layer of the vertex detector in the case of TESLA with high luminosity parameters. In the plot the angular coverage of the layer was kept constant

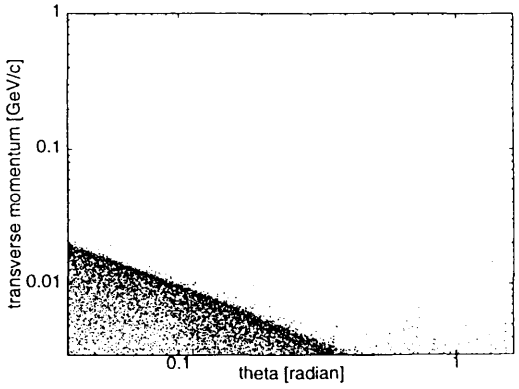

Figure 3: The final angle and transverse momentum of the particles from pair production in the case of TESLA.

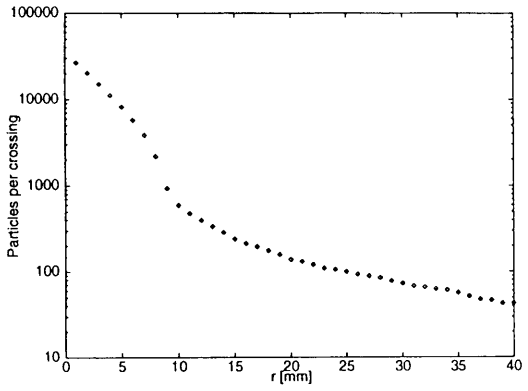

Figure 4: The number of particles that hit the vertex detector as a function of the radius of its inner layer. The magnetic field was assumed to be $B_z = 3\,\mathrm{T}$ and the opening angle of the detector $\theta_0 = 200\,\mathrm{mradian}$.

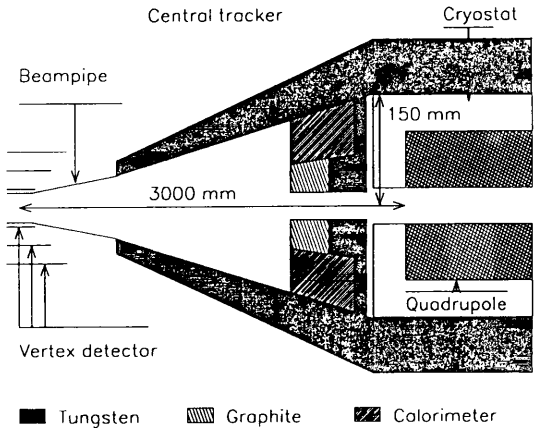

Figure 5: The layout of the mask in the detector of TESLA.

at $\cos\theta = 0.98$ but the radius was varied. The magnetic field in the detector was assumed to be $B_z = 3\,\mathrm{T}$ as foreseen in Reference [11]. Below a certain radius the number of particles rises drastically. This is because the detector is not only hit by the particles that started with a large angle and transverse momentum but also those that received their transverse momentum and their angle from the deflection by the beams. Using a smaller coverage (larger dead angle) or stronger magnetic field allows a smaller radius.

For TESLA, it is foreseen to have the innermost layer of the vertex detector at a radius $r = 25\,\mathrm{mm}$. Particles can cause more than one hit since they travel along a helix. Using a GEANT based simulation, the hit density found is about $10^{-2}\,\mathrm{mm}^{-2}$ for the reference parameters (including a patch factor 1.5 to account for the difference between the Vermaseren Monte-Carlo and GUINEA-PIG). With the high luminosity parameters one finds a hit density of about $1.5 \cdot 10^{-2}\,\mathrm{mm}^{-2}$.

Also the particles that are not directly entering the vertex detector can cause background. These particles hit the final quadrupoles on both sides of the detector. The detector can be shielded from the backscattering photons by a tungsten mask as shown in Fig. 5. The charged low energy particles that are backscattered are however led by the main detector field back into the vertex detector—causing an increase in the number of hits by an order of magnitude. This can be prevented by adding an additional inner mask inside the main one. This consists of a tungsten layer towards the outside of the detector and a low-Z material towards the inside. The radius of the opening in this mask has to be smaller than the beam pipe to be effective.

8 LUMINOSITY MONITOR

One of the important problems in a linear collider is to adjust the beams in the collision point to achieve highest luminosity. Beam-beam deflection scans have been used to this end at the SLC. During this scan however the luminosity production is interrupted.

Three different processes could be used to optimise the collision during luminosity production in future linear colliders [14], namely the bremsstrahlung, beamstrahlung and pair production.

The bremsstrahlung process has the advantage that the event rates are directly proportional to the luminosity except for the beam size effect, which has only a weak dependence on vertical spot size. Either the hard photons or the remnant beam particles which lost a significant amount of energy could be detected in principle. The photon will be accompanied by a large number of softer photons from the beamstrahlung process, so the detector needs to be able to detect only photons above a fixed threshold energy. It seems therefore simpler to detect the low energy remnant particles. Here one has to avoid detecting particles which lost energy due to beamstrahlung or the low energy particles from pair production. As Fig. 6 shows, this is possible around $E = 50\,\mathrm{GeV}$ in the case of TESLA with high luminosity parameters. For CLIC at 3 TeV, the bremsstrahlung signal is completely hidden in that of the spent beam, see Fig. 7. One therefore has to find other means to tune the luminosity.

In case of the high luminosity TESLA, the particles from the pair production will deposit about 12 TeV in the inner mask shown in Fig. 5. The measurement of this energy provides a signal which allows the luminosity to be tuned. The most frequent parameter to tune is the vertical waist of the two beams. Figure 8 shows the luminosity and energy deposited per bunch crossing in the two inner masks if one varies the waist of one of the beams. The other beam is assumed to be at the optimal waist position. The luminosity found from the scan of 20 bunch crossings is lower by a fraction of $4 \cdot 10^{-4}$ than the optimum one.

9 THE TOP QUARK THRESHOLD SCAN

Measuring the top production cross section around threshold is useful for determining the top mass m_t, the strong coupling constant α_S and the top width Γ_t [15]. The cross section is affected by initial state radiation, the energy spread in the beams and the beamstrahlung. The

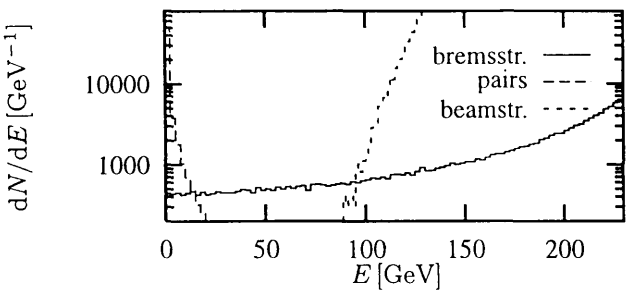

Figure 6: The low energy particle spectra for the TESLA parameters due to the pair production, bremsstrahlung and beamstrahlung.

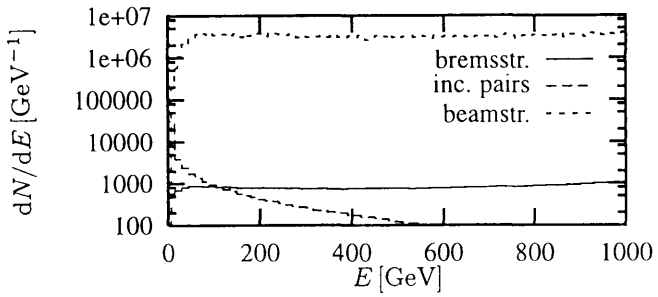

Figure 7: The low energy particle spectra for the CLIC parameters at 3 TeV.

initial state radiation is unavoidable while the other two parameters depend on the machine design. Comparison of TESLA, SBLC and NLC [1] showed some difference which is however not very large.

In Fig. 9 the $\Delta\chi^2 = 1$ contour of the top scan using nine points is shown in m_t and Γ_t for fixed α_S. An integrated luminosity of 50 fb^{-1} [15] and the reference parameters of TESLA were assumed. The outer curve corresponds to a background rate three times larger than predicted.

10 CONCLUSION

Disruption and beamstrahlung have important effects on the total luminosity and its spectrum in linear colliders. The presented program simulates these and the resulting electro-magnetic and hadronic background. The program was used to evaluate the precision achievable in physics experiments due to smearing of the luminosity spectrum and the background. Possibilities for optimising the luminosity were studied, predicting good results.

11 REFERENCES

[1] D. Schulte. TESLA-97-08 (1996)

[2] E-mail address: Daniel.Schulte@CERN.CH

[3] G. L. Kotkin, V. G. Serbo, and A. Schiller. Int. J. Mod Phys. A, **7** (1992) 4707–4745.

[4] A. E. Blinov and 15 co-authors. Phys. Lett. B, **113** (1982) 423.

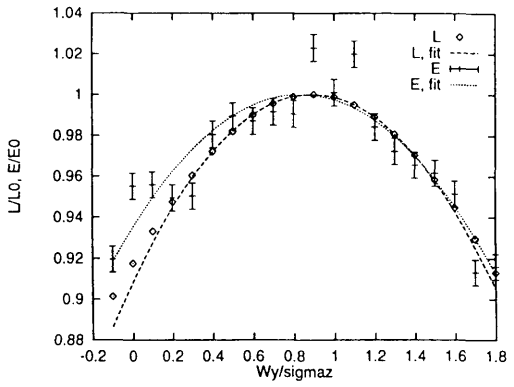

Figure 8: The luminosity and the energy deposited by the particles from pair creation in the inner masks. The position of the vertical waist of one of the beams was varied while the waist of the other beam was in optimal position.

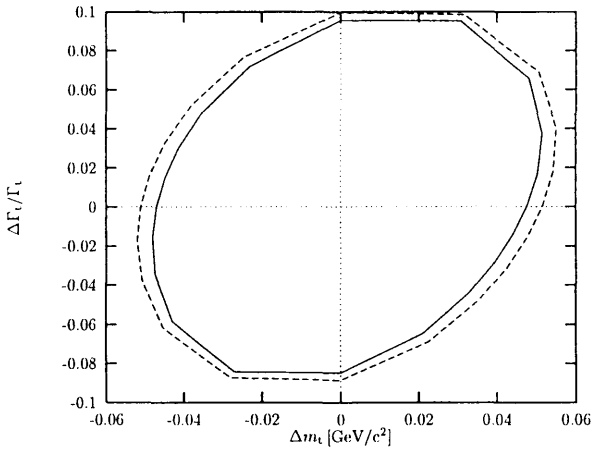

Figure 9: The resolution of the top threshold scan.

[5] K. Piotrzkowski. DESY 95-051 (1995).

[6] V. N. Baier and V. M. Katkov. Sov. Phys. Dokl., **17** (1973) 1068.

[7] G. A. Schuler and T. Sjöstrand. Z. Phys. C, **37** (1997) 677–688.

[8] P. Chen and M. E. Peskin. SLAC-PUB-5873 (1992).

[9] J. R. Forshaw and J. K. Storrow. Phys. Lett.B, **268** (1991) 116–121.

[10] T. Sjöstrand. Comp. Phys. Comm., **82** (1994) 74-90.

[11] R. Brinkmann, G. Materlik, J. Rossbach and A. Wagner (editors). ECFA 1997-182

[12] M. Drees and K. Grassie. Z. Phys. C, **28** (1985) 451–462.

[13] M. Glück, E. Reya, and A. Vogt. Physical Review D, **46** (1992) 1973.

[14] O. Napoly and D. Schulte. Linac 98.

[15] A. Juste, M. Martinez and D. Schulte. DESY-97-123-E (1997)